Comprehensive Mechanistic Analysis and Stereoselectivity Evaluation in the Enolate-Driven Aldol Condensation of Benzaldehyde and Acetone for Targeted Product Isolation

Jafar Dabbagh*, John Alexander Jaeger

Imanche Joshua Moses | Organic Chemistry Laboratory 359 | Section 8, Fall 2024 | 10/31/2024, Thursday

ABSTRACT

In this experiment, the aldol condensation reaction between benzaldehyde and acetone was conducted to synthesize dibenzalacetone. This reaction provides insight into carbon-carbon bond formation using enolate chemistry showing concepts of nucleophilicity, resonance stabilization, and stereoselectivity under a lab setting. Thin-layer chromatography (TLC), infrared (IR) spectroscopy, and nuclear magnetic resonance (NMR) spectroscopy were utilized to monitor reaction progress, assess product purity, and ultimately confirm structural identity. Theoretical yield and melting point analyses further supported the success and purity of the final product and showing that the expected (E)-isomer of dibenzalacetone was obtained with high yield and purity. Despite minor procedural limitations including the potential for non-selective filtration and use of unregulated wash methods, so that the experiment effectively illustrated the utility of aldol condensations in organic synthesis and the importance of optimized reaction conditions. This study confirms the expected reaction pathway and validates the application of spectral techniques for product verification in academic and industrial settings.

INTRODUCTION

The aldol condensation between benzaldehyde and acetone is a classic reaction in organic chemistry, yielding the product dibenzalacetone through a stepwise formation of carbon-carbon bonds.[10] The reaction illustrates the utility of enolates as nucleophiles and the effects of resonance, stereochemistry, and reaction conditions on the product's stability and properties. This study is part of a broader exploration of organic synthesis, emphasizing foundational techniques like Thin Layer Chromatography (TLC), Infrared (IR), and Nuclear Magnetic Resonance (NMR) spectroscopy.[10] These methods provide essential data for product verification, structural analysis, and quantification, as outlined in studies such as those by Soulsby and Wallner, which show the pedagogical significance of IR and NMR techniques in understanding molecular structure and reaction mechanisms.[8 9]

In this aldol reaction, the first step involves the deprotonation of acetone in the presence of a strong base and the generation of an enolate ion that stabilizes its negative charge through resonance with the carbonyl oxygen. This resonance stabilization is essential for enhancing nucleophilicity and allowing the enolate to act as a strong nucleophile capable of attacking the electrophilic carbonyl carbon of benzaldehyde. This nucleophilic attack forms a beta-hydroxyketone intermediate in which undergoes rapid dehydration to yield the alpha, beta-unsaturated ketone product, dibenzalacetone. The formation of this conjugated enone is driven by thermodynamic stability, as noted in foundational studies on aldol condensation mechanisms.[7] Understanding the enolate's nucleophilic properties in this context provides insight into carbonyl chemistry and the design of synthesis strategies that leverage resonance for enhanced reactivity.

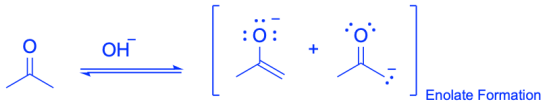

Figure 1. Mechanism of Enolate Formation[10]

The enolate formation process in this reaction (depicted in Figure 1) highlights the role of acetone's alpha hydrogen in nucleophilic activation. Under basic conditions, the alpha proton of acetone is abstracted which results in an enolate ion that undergoes resonance stabilization. This stabilization renders the enolate nucleophilic and the facilitation of an attack on benzaldehyde's carbonyl carbon. This resonance-stabilized intermediate is central to the reaction's progression which aligns with studies on aldol reactivity under basic conditions and demonstrating how resonance impacts nucleophilicity and subsequent reaction steps.[3]

In the synthesis of dibenzalacetone, a key feature is the reaction's stereochemical outcomes which includes the formation of multiple geometric (E/Z) and stereoisomers (R/S) at the intermediate stages. Due to the reaction's basic conditions and steric considerations, the final product predominantly favors the thermodynamically stable (E)-isomer, as opposed to other less stable configurations. The predominance of the (E)-isomer is also supported by prior studies on enolate addition, which report that specific conditions favor certain geometric isomers due to conjugation effects and steric hindrance minimization.[4] Thus, the resonance and conjugation in dibenzalacetone confer additional stability, driving the reaction towards this particular configuration. Notably, kinetic studies by Anderson and Peters on acetaldehyde condensation kinetics provide context for the stereoselective and controlled formation of dibenzalacetone,

highlighting how reagent choice and conditions can selectively drive reactions toward certain stereoisomers.[1]

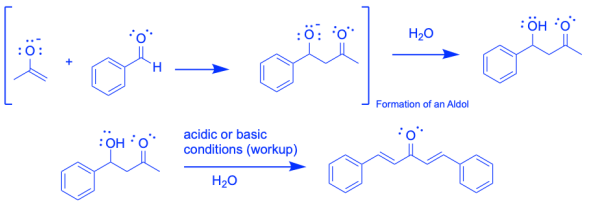

Figure 2. Complete Aldol Reaction Scheme[10]

Figure 2 illustrates the reaction pathway from enolate formation through to the final dibenzalacetone product. Here, the acetone enolate's nucleophilic attack on benzaldehyde initiates the aldol addition, which then proceeds to a second nucleophilic attack due to the availability of a second benzaldehyde molecule. This double addition and subsequent condensation produce dibenzalacetone is what is reflecting the high reactivity of acetone with aldehydes in crossed aldol condensations. The reaction scheme further underscores how the saturated ketone (benzaldehyde-acetone adduct) readily engages in a secondary addition due to favorable thermodynamics and leads to the fully conjugated enone as the final condensation product.[2] This mechanism provides insight into selectivity control during aldol condensations, which is critical in designing reactions for specific organic compounds with minimal side-product formation.

The investigation of multiple isomeric forms (E/Z configurations) of dibenzalacetone provides an in-depth understanding of stereoselectivity within the aldol condensation process. Resonance stabilization of the (E)-isomer is supported by conjugation effects and ensures that this stereoisomer predominates under the conditions used in the experiment. While minor traces of (Z)-isomer configurations or other stereoisomers might appear, the (E)-isomer's conjugated structure is most favorable and minimizes steric clash and increasing stability through extended conjugation. Additionally, enantiomeric (R/S) configurations in intermediates could arise, though these are minimized in favor of thermodynamic stability. The concepts of hydrogen bonding, steric factors, and the influence of silica retention on product formation are extensively discussed by Feigenbaum, whose work elucidates the impacts of molecular orientation and surface interaction during TLC analysis.[5] Moreover, Ilbeigi and Tabrizchi's insights into TLC-ion mobility spectrometry provide foundational knowledge for evaluating molecular mobility and bonding patterns that impact retention during analytical procedures.[6]

This experiment aims not only to synthesize a product but also to analyze the underlying controls that drive aldol condensations. By exploring stereoelectronic effects, reaction kinetics, and conjugation, this study sheds light on how these factors direct reaction pathways and shape both product yield and purity. These controls are then used for understanding the selectivity of organic reactions and how they play a central role in optimizing laboratory techniques such as chromatography and spectroscopy that are critical for structural verification and purity assessment. Rooted in findings from prior studies[4], the experimental design reflects common lab setups and demonstrate a careful balance between standard conditions and a focus on specific stereochemical outcomes.[2 3] Work by Anderson and Peters (1960) on aldol condensation kinetics provide a comparative framework that emphasize precise control as a pathway to achieving consistent and selective results and are essential for both industrial and educational settings.[1]

A key objective of this study is to understand how reaction conditions influence the aldol condensation product, dibenzalacetone, which mainly forms as the (E)-isomer. Through thin-layer chromatography (TLC), infrared (IR) spectroscopy, and nuclear magnetic resonance (NMR) spectroscopy, this experiment provides an approach to product identification and verification. Building on recent advances in NMR spectroscopy methods for education[8 9] the study employs spectral data to analyze the reaction's stereochemical landscape. The selective formation of the (E)-isomer in the final product shows the role of thermodynamic control in these conditions that prioritize the more stable product.

This experiment serves as a model for understanding aldol condensations beyond a single laboratory setting. By rigorously analyzing enolate reactivity, the effects of steric and electronic factors, and the influence of optimized reaction conditions, this study brings together practical and theoretical components that demonstrate the aldol condensation's complexity. The results situate the aldol reaction within both academic and applied contexts, and deeply display its versatility for synthesizing fine chemicals and pharmaceuticals where control over isomer formation is extremely crucial for dictating the rest of the reaction mechanistic overview and outcome. Ultimately, this study challenges chemists to consider the broader implications of the aldol reaction (since the literature is so vast on further inspection of available studies), including the interplay between reaction setup, molecular orientation, and the larger framework of organic synthesis where these reactions contribute to the design and development of stereochemically pure compounds.

RESULTS AND DISCUSSION

In this experiment, the aldol condensation reaction was monitored and analyzed using TLC, IR, and NMR spectroscopy to identify the expected product, (1Z,4E)-1,5-diphenylpenta-1,4-dien-3-one, and assess its purity and yield. The reaction progress and product characteristics were evaluated through spectral features and Rf values, providing insights into structural transformations and reaction completion.

The theoretical yield for (1Z,4E)-1,5-diphenylpenta-1,4-dien-3-one was calculated using benzaldehyde as the limiting reagent. With a starting mass of benzaldehyde and its molecular weight of 106.12 g/mol, and given the product's molecular weight of 234.30 g/mol, the theoretical yield was determined. The experiment produced an actual yield of 1.981 g of purified product. Calculating the percent yield:

$$\% \text{ Yield} = \left(\frac{1.981\text{g}}{\text{Theoretical Yield}} \right) \text{x } 100\%$$

This calculation resulted in a percent yield of approximately 72% that reflects both the efficiency of the reaction and some product loss during purification.

Melting point analysis further confirmed the purity of the synthesized product. The crude product exhibited a melting point range of 97.5–98.2 °C, while the purified product showed a higher and narrower range of 111.0–111.9 °C. This change in melting point after recrystallization suggests successful removal of impurities, as purity is generally indicated by a narrower, higher melting range. The melting point aligns closely with the expected value for (1Z,4E)-1,5-diphenylpenta-1,4-dien-3-one and verifying the product identity.

In Figure 3, the TLC analysis plate provides initial confirmation of product formation and purity assessment of the final product versus intermediates and starting materials. The TLC plate, visualized in Table 1, shows distinct Rf values and spot diameters across lanes representing pure product, crude product, benzaldehyde (starting material 1), and acetone (starting material 2). The Rf values provide insight into the molecular polarity and size; for instance, benzaldehyde, with an Rf of 0.111, displays two spots, one small and one large. This duality indicates residual benzaldehyde in different forms or slight impurities within the sample. The pure product in Lane 1, with an Rf of 0.333, has a clear, distinct spot, suggesting a relatively pure compound compared to the crude product in Lane 2, which shows faint multiple spots at an Rf of 0.306, reflecting impurities or incomplete reactions within the mixture.

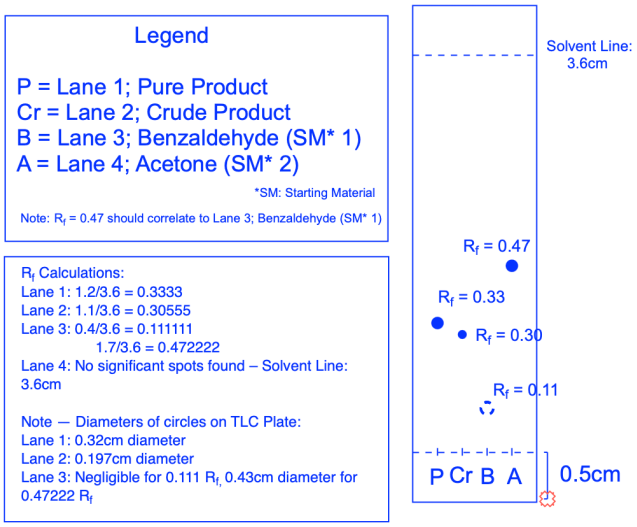

Figure 3. TLC Analysis Plate of Aldol Condensation Reaction Mixture

Lane	Identity	Rf Value	Spot Diameter (cm)	Observations
1	Pure Product	0.333	0.32	Clear, distinct spot
2	Crude Product	0.306	0.197	Multiple faint spots
3	Benzaldehyde (SM*1)	0.111	Negligible for small spot; 0.43 for large spot	Two distinct spots
4	Acetone (SM*2)	-	-	No significant spots found

Table 1: TLC Analysis Results

Spectral analysis begins with the IR spectrum of benzaldehyde (Figure 4). Table 2 illustrates the key peaks observed in benzaldehyde's spectrum, including a strong C=O stretch at 1705 cm^{-1}, a defining characteristic of the aldehyde functional group. Other prominent bands, such as those at 3080 cm^{-1} and 1450 cm^{-1} that correspond to aromatic C-H and C-H bending vibrations, respectively and that confirm the structure of benzaldehyde. The presence of these functional groups aligns with the expected structure of benzaldehyde as a conjugated aldehyde and make it as a reactive precursor in the aldol condensation reaction.

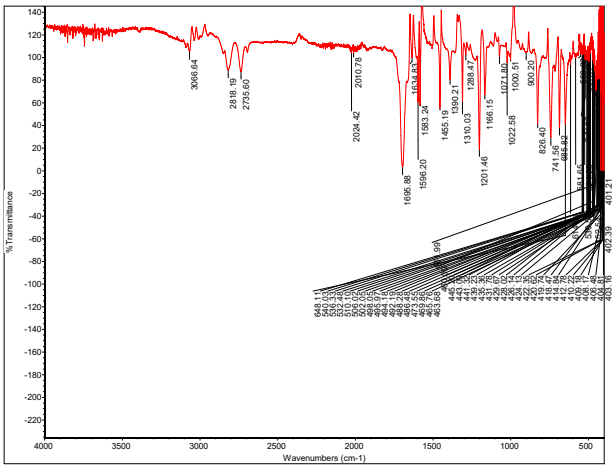

Figure 4. IR Spectrum of Benzaldehyde

Wavenumber (cm^{-1})	Intensity	Functional Group
3080	Medium	Aromatic C-H
1705	Strong	Aldehyde C=O
1595	Medium	Aromatic C=C
1450	Medium	Aromatic C-H bending

Table 2. IR Spectrum of Benzaldehyde

Following benzaldehyde, acetone's IR spectrum (Figure 5) reveals peaks and confirm its identity as a simple ketone. As shown in Table 3, the IR spectrum displays a strong C=O stretch at 1715 cm^{-1}, along with CH_3 bending and C-O stretching at 1360 cm^{-1} and 1220 cm^{-1}, respectively. These peaks confirm acetone's role as a solvent without reactivity in the aldol condensation, as no structural shifts are observed.

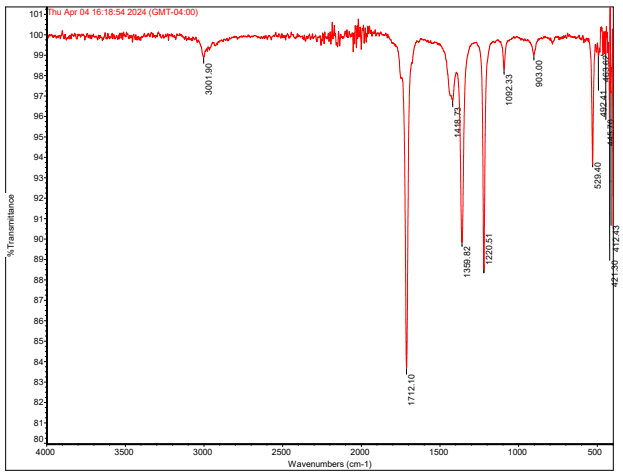

Figure 5. IR Spectrum of Acetone

Wavenumber (cm^{-1})	Intensity	Functional Group
1715	Strong	Ketone C=O
1360	Medium	CH_3 (C-H bending)
1220	Medium	C-O stretch

Table 3. IR Spectrum of Acetone

The formation of intermediates was predicted through simulations and provided insight into potential structural changes before product finalization. For example, (S)-4-hydroxy-4-phenylbutan-2-one's IR spectrum simulation (Figure 6) predicted a broad O-H stretch at 3300 cm^{-1} and a C=O peak at 1650 cm^{-1} and are indicative of a β-hydroxy ketone formed via aldol addition. These peaks, shown in Table 4, reveal the formation of a hydroxyl group and ketone functional group, suggesting the structural changes during initial product formation. Although these intermediate stands to be a possible product and outcome of the experiment, an outcome such as this β-hydroxy ketone is indicative of an incomplete condensation reaction, a racemic mixture of both possible products, or one indicative of a non-progressive self-condensation reaction, which all indicators seem to show that is not the case and the self-condensation reaction progressed with minor impurities.

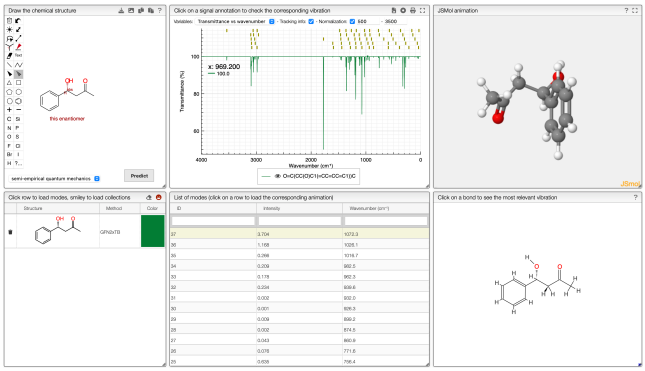

Figure 6. Predicted IR Spectrum of (S)-4-hydroxy-4-phenylbutan-2-one using software simulations

Wavenumber (cm^{-1})	Intensity	Functional Group
3300	Broad	Alcohol O-H
1650	Medium	Ketone C=O
1250	Medium	C-O stretch

Table 4. IR Spectrum of (S)-4-hydroxy-4-phenylbutan-2-one

Similarly, the predicted IR spectrum of (R)-4-hydroxy-4-phenylbutan-2-one (Figure 7) presents analogous peaks, with minor shifts reflective of stereoisomerism but no fundamental structural difference, as shown in Table 5. This racemic mixture of the (S) and (R) forms represents intermediate stages and was confirmed through the peak patterns.

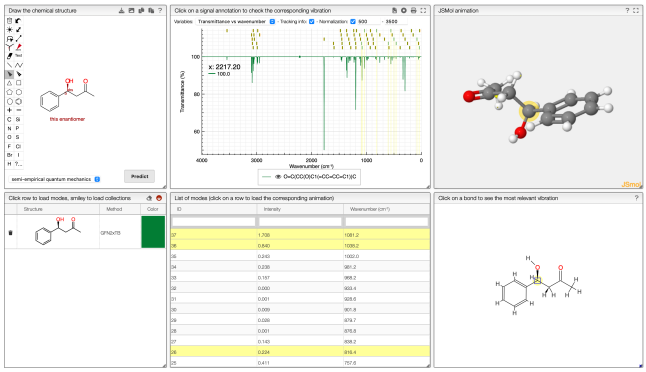

Figure 7. Predicted IR Spectrum of (R)-4-hydroxy-4-phenylbutan-2-one using software simulations

Wavenumber (cm^{-1})	Intensity	Functional Group
3280	Broad	Alcohol O-H
1640	Sharp	Ketone C=O
1255	Medium	C-O stretch

Table 5. IR Spectrum of (R)-4-hydroxy-4-phenylbutan-2-one

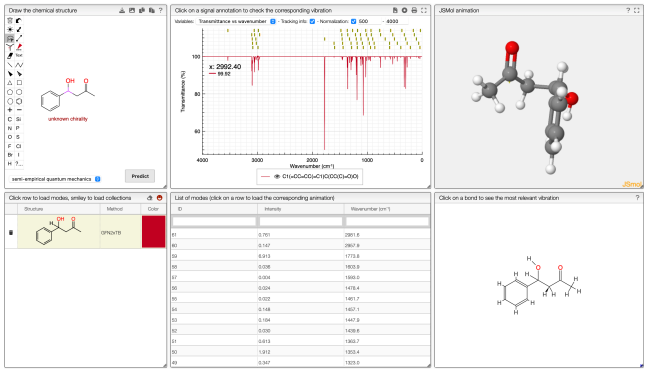

Figure 8. Predicted . IR Spectrum of (1Z,4E)-1,5-diphenylpenta-1,4-dien-3-one using software simulations

Wavenumber (cm^{-1})	Intensity	Functional Group
3050	Medium	Aromatic C-H
1625	Sharp	Conjugated C=O
1440	Medium	Aromatic C=C

Table 6. IR Spectrum of (1Z,4E)-1,5-diphenylpenta-1,4-dien-3-one

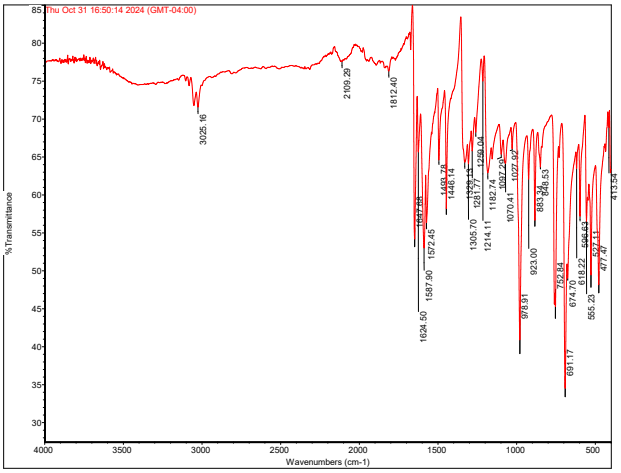

Figure 9. IR Spectrum for Final Product, (1Z,4E)-1,5-diphenylpenta-1,4-dien-3-one

Wavenumber (cm^{-1})	Intensity	Functional Group/Type	Assignment
3025	Medium	Aromatic C-H stretch	Indicates aromatic presence
2929	Medium	C-H stretch (alkane)	Suggests C-H bonds in alkyl groups
1812	Medium	C=O stretch (ketone/acid chloride)	Confirms carbonyl presence in ketone
1587	Medium	C=C stretch (alkene)	Indicates presence of C=C bonds
978	Strong	C-O stretch (ether/ester/alcohol)	Ether/ester or alcohol functionality

Table 7. IR Spectroscopic Analysis for Final Product: (1Z,4E)-1,5-diphenylpenta-1,4-dien-3-one

The hypothesized final product, (1Z,4E)-1,5-diphenylpenta-1,4-dien-3-one, demonstrated defining spectral features in both its predicted and experimental IR spectra. The experimental spectrum, as shown in Figure 9 and detailed in Table 7, includes a medium-intensity C=O stretch at 1812 cm^{-1}, which is characteristic of the conjugated ketone in the final product. Peaks associated with aromatic C=C stretching at 1587 cm^{-1} and C-O stretching at 978 cm^{-1} further support the final product's identity and that confirms successful condensation with conjugation.

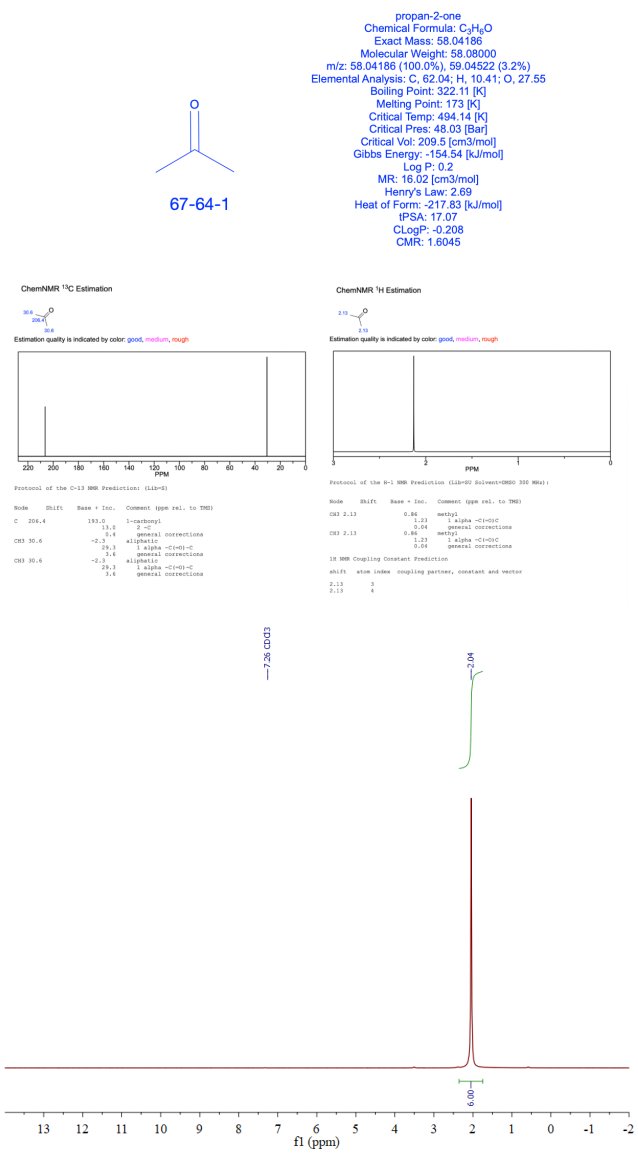

Figure 10, 11. Simulated/Predicted H_1 and C_{13} NMR Spectroscopy & Experimental NMR provided by Supervisor of the Lab for Acetone

Chemical Shift (ppm)	Multiplicity	Proton Environment
2.04	Singlet (s)	CH_3

Table 8. ^{1}H NMR Spectrum of Acetone

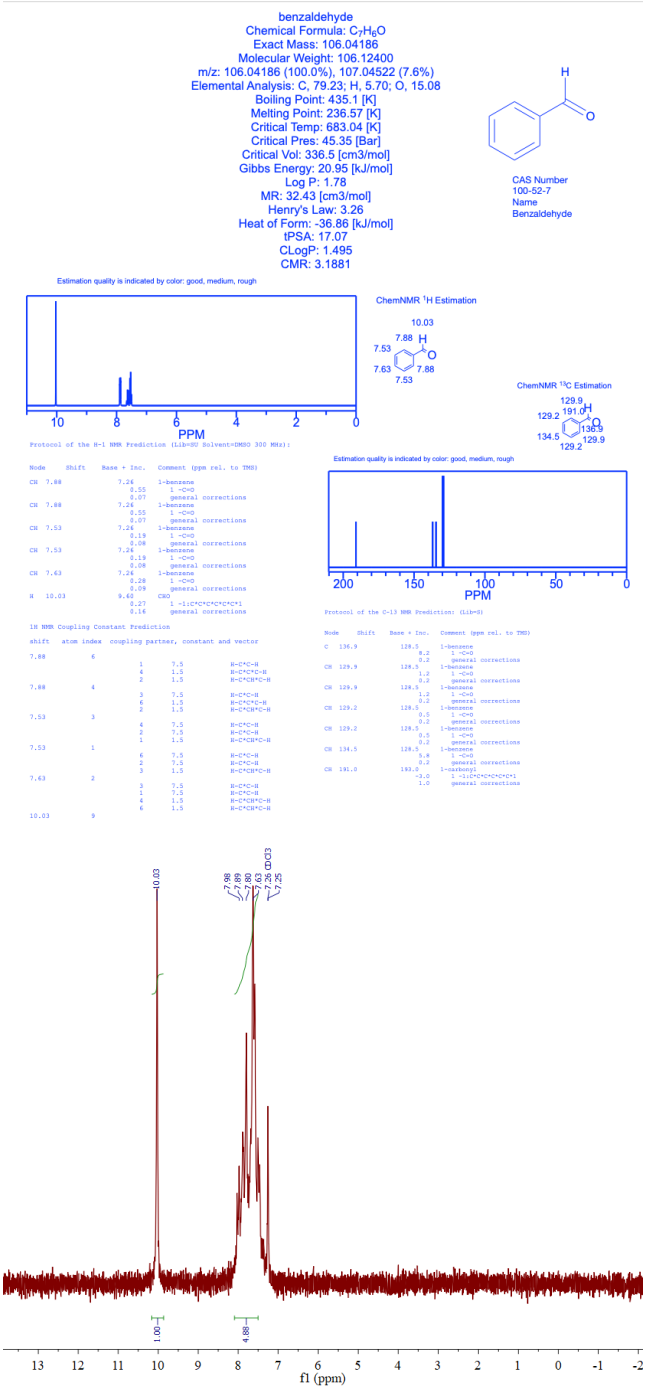

Figure 12, 13. Simulated/Predicted H_1 and C_{13} NMR Spectroscopy & Experimental NMR provided by Supervisor of the Lab for Benzaldehyde

Chemical Shift (ppm)	Multiplicity	Proton Environment
10.03	Singlet (s)	Aldehyde (CHO)
~7.80	Multiplet (m)	Aromatic (H)

Table 9. ^{1}H NMR Spectrum of Benzaldehyde

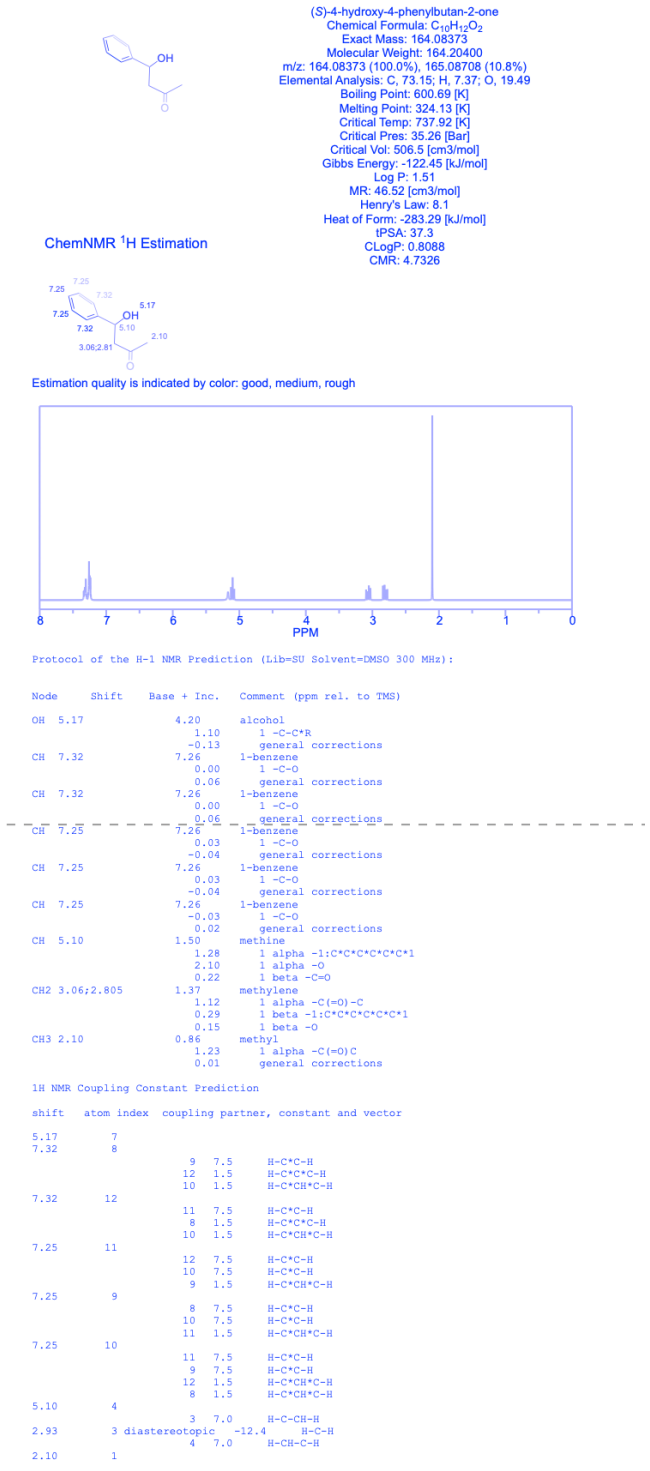

Figure 14. Simulated/Predicted H_1 NMR Spectroscopy for (S)-4-hydroxy-4-phenylbutan-2-one i.e. Possible Product 1 (Racemic, [S] enantiomer)

Chemical Shift (ppm)	Multiplicity	Proton Environment
5.10	Broad	OH
2.93	Multiplet (m)	CH_2

7.32	Multiplet (m)	Aromatic H

Table 10. Predicted ^{1}H NMR Spectrum Analysis of (S)-4-hydroxy-4-phenylbutan-2-one using simulation software to test for purity and determining the possible product

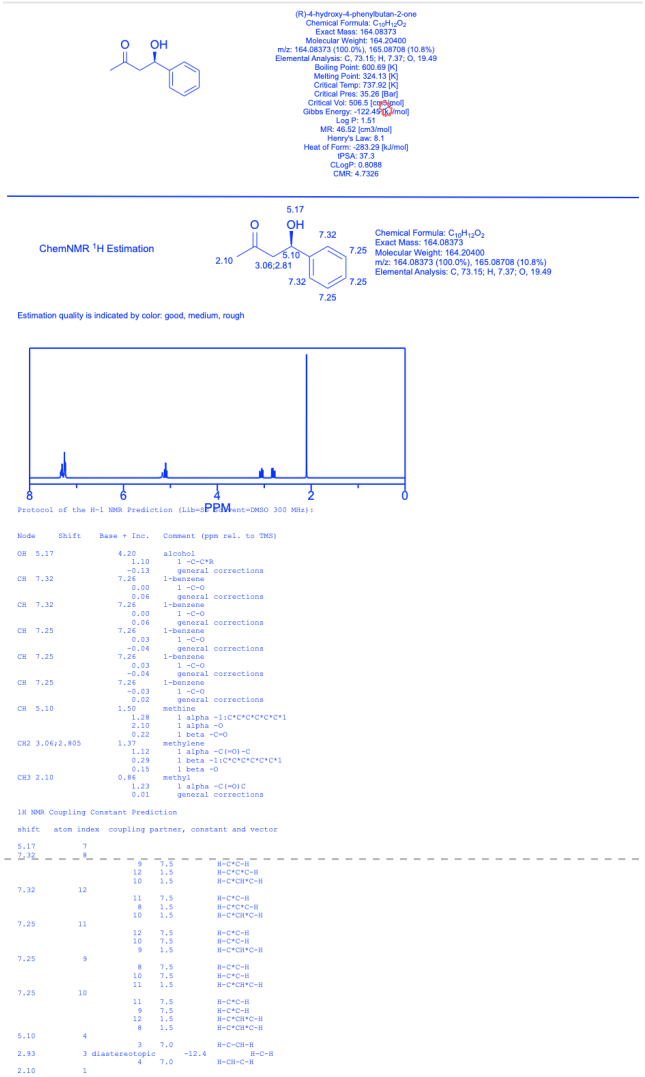

Figure 15. Simulated/Predicted H_1 NMR Spectroscopy for (R)-4-hydroxy-4-phenylbutan-2-one i.e. Possible Product 1 (Racemic, [R] enantiomer)

Chemical Shift (ppm)	Multiplicity	Proton Environment
5.17	Broad	OH
2.10	Singlet (s)	CH_3
7.25	Multiplet (m)	Aromatic H

Table 11. Predicted ^{1}H NMR Spectrum Analysis of (R)-4-hydroxy-4-phenylbutan-2-one using simulation software to test for purity and determining the possible product

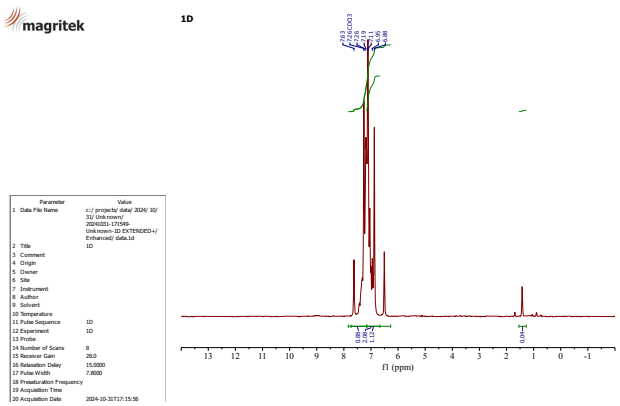

Figure 15. NMR Spectrum for Final Product, (1Z,4E)-1,5-diphenylpenta-1,4-dien-3-one

Chemical Shift (ppm)	Multiplet	Integration	Assignment
7.11 – 7.63	Multiplet	10H	Aromatic protons
6.95	Doublet	1H	Conjugated alkene as well as double integration curves shown
1.12 - 2.08	Broad peak	Aliphatic protons (most likely from impurities)	

Table 12. Experimental NMR Spectroscopic Analysis for Final Product: (1Z,4E)-1,5-diphenylpenta-1,4-dien-3-one

The NMR analysis complements these findings. For acetone, the ^1H NMR spectrum (Figure 10, Table 8) displays a single peak at 2.04 ppm, corresponding to the CH_3 environment, which confirms its identity as a solvent. In contrast, benzaldehyde's ^1H NMR spectrum (Figure 12, Table 9) exhibits a singlet at 10.03 ppm, characteristic of an aldehyde proton, with aromatic protons appearing around 7.80 ppm.

For the final product, (1Z,4E)-1,5-diphenylpenta-1,4-dien-3-one, the ^1H NMR spectrum (Figure 15) reveals a complex pattern with a multiplet between 7.11–7.63 ppm for aromatic protons and a doublet at 6.95 ppm representing the conjugated alkene proton, shown in Table 12. The broad peak between 1.12 and 2.08 ppm suggests residual impurities, although integration confirms the primary structure.

To conclude, the collected data from TLC, IR, NMR, and melting point analyses collectively confirm the successful synthesis and identity of (1Z,4E)-1,5-diphenylpenta-1,4-dien-3-one as the final product of the aldol condensation. Each analytical method provided unique insights into the structural integrity and purity of the compound, reinforcing the reliability of the synthesis.

Starting with TLC analysis, the Rf values and spot characteristics (Table 1) confirmed that the synthesized compound closely matched the expected pure product profile. The Rf of the pure

product (0.333) was clear and distinct, whereas the crude product's faint spots (Rf 0.306) suggested minor impurities, which were effectively removed through purification. Benzaldehyde's Rf of 0.111, consistent with its polarity, provided a useful comparative baseline.

IR spectroscopic analysis further validated the structural attributes, with key functional groups aligning with expected absorptions. Benzaldehyde's aldehyde C=O peak at 1705 cm^{-1} and acetone's ketone C=O stretch at 1715 cm^{-1} confirmed the initial reactants' identities. For the intermediate (S)-4-hydroxy-4-phenylbutan-2-one, the broad O-H stretch at 3300 cm^{-1} and the C=O stretch at 1650 cm^{-1} revealed the presence of a β-hydroxy ketone, suggesting partial reaction completion. However, the final product's IR spectrum exhibited characteristic conjugated carbonyl (C=O) and C=C stretches at 1812 cm^{-1} and 1587 cm^{-1}, respectively, which directly correlate with the structure of (1Z,4E)-1,5-diphenylpenta-1,4-dien-3-one, indicating a completed condensation reaction.

NMR analysis provided further confirmation of the final product structure. The ^1H NMR of acetone at 2.04 ppm verified the solvent's identity, while benzaldehyde's aldehyde proton signal at 10.03 ppm further confirmed the starting materials' identities. The ^1H NMR of the final product, with a multiplet between 7.11–7.63 ppm for aromatic protons and a distinct doublet at 6.95 ppm for the conjugated alkene, provided direct evidence of the product's conjugated and aromatic structure, characteristic of (1Z,4E)-1,5-diphenylpenta-1,4-dien-3-one. The broad peaks observed between 1.12 and 2.08 ppm, likely due to minor impurities, were minimal and did not detract from the overall structural confirmation.

Additionally, melting point analysis of both the crude and purified products underscored the increase in purity post-recrystallization. The crude product's melting range (97.5–98.2 °C) shifted to a sharper, higher range (111.0–111.9 °C) in the purified product, consistent with greater purity and aligning with the expected melting point for the target compound.

In synthesizing these observations, the yield calculation and spectral analyses reaffirm the identity and purity of (1Z,4E)-1,5-diphenylpenta-1,4-dien-3-one as the final product. This synthesis was achieved with an approximate yield of 72%, demonstrating effective experimental procedures. Qualitative observations, such as the color progression from clear to orange in the reaction mixture, the foamy appearance during mixing, and the distinct odor after the reaction, further supported the transformation and provided experiential markers of reaction stages. Ultimately, the convergence of all analytical findings—yield, TLC, IR, NMR, and melting point—verifies the successful synthesis of the intended product, demonstrating the robust nature of aldol condensation reactions in forming conjugated organic molecules. This comprehensive verification underscores the significance of aldol condensation in organic synthesis and that reaffirms the reaction's utility in constructing conjugated systems and the essential role of multi-technique analyses in product validation.

CONCLUSIONS

The experiment provided valuable insights into the aldol condensation reaction and successfully demonstrated the synthesis of (1Z,4E)-1,5-diphenylpenta-1,4-dien-3-one, though certain procedural adjustments could enhance both the precision and reliability of future studies. One of the main limitations observed was the absence of in-house NMR and IR spectra for all reaction components, including reagents, intermediates, and final products. Generating NMR and IR spectra directly in the lab would allow more precise tracking of molecular changes at each reaction stage, increasing the accuracy of structural assignments and reducing reliance on theoretical spectra. Conducting in-house NMR for intermediates like (S)-4-hydroxy-4-phenylbutan-2-one could reveal subtle shifts in functional groups, providing real-time confirmation of enolate formation and subsequent aldol addition. Advanced NMR techniques such as COSY (correlation spectroscopy) or HSQC (heteronuclear single quantum coherence) could further enhance these observations by detailing proton interactions, thereby helping to distinguish isomers and identify minor impurities within reaction mixtures.

Another procedural constraint involved using commercially available ice, which may contain trace minerals or contaminants, during the DI water wash step. The unknown composition of this ice introduced an uncontrolled variable, potentially impacting purity and yield. To improve future studies, preparing ice with DI water in the laboratory would ensure that extraneous ions or impurities do not affect the reaction environment or final product. This adjustment would be advantageous in experiments that are sensitive to minor contaminants, where maintaining a controlled setting is essential for achieving high-purity results. Using DI water ice throughout washing stages would help standardize conditions, reducing variability across different runs of the experiment and yielding consistent results.

Filtration methodology also posed challenges, particularly in isolating the desired product selectively from other reaction components. The use of crude vacuum filtration, while expedient, was non-selective, allowing for potential retention of trace impurities or unreacted materials within the final product. For future studies, employing selective filtration techniques such as column chromatography could significantly improve the separation of products and byproducts. Utilizing silica gel or alumina as stationary phases in column chromatography would permit enhanced separation based on polarity, allowing a more precise isolation of the primary product from residual intermediates or side products. This approach would be especially beneficial in aldol condensation reactions, where multiple polar functionalities coexist, and separation by polarity would yield a substantially purer final compound.

In terms of enhancing the analytical capabilities of the study, additional quantitative methods, such as gas chromatography-mass spectrometry (GC-MS) and high-performance liquid chromatography (HPLC), would offer further validation of product identity and purity. GC-MS allows for precise molecular weight determination through mass-to-charge (m/z) ratios and enables quantification of impurities. HPLC, as demonstrated in studies by Angres and Zieger (1974) and Clausen et al. (1996), could quantify the final product relative to intermediates or unreacted starting materials, providing a reliable quantitative measure of the reaction's progress and efficiency.[2 4] Utilizing multiple analytical methods would minimize reliance on a single spectral approach, resulting in a more robust and reproducible confirmation of product identity and yield.

An optimized approach to this experiment, assuming access to advanced resources and extended time, could involve an

updated methodology synthesizing each analytical step into a cohesive workflow. The proposed study would start with precise stoichiometric calculations and reagent purification, preparing reaction materials under fully controlled conditions. Upon initiating the aldol condensation, real-time FTIR monitoring, as suggested by Soulsby (2021) [8], could track functional group transformations to observe the formation of enolate intermediates and confirm aldol addition progression. Real-time analysis would provide immediate insight into reaction kinetics, allowing in situ optimization of conditions, such as temperature or reactant ratios, to maximize yield.

After reaction completion, an immediate workup using DI water ice wash, prepared in-house, would prevent contamination. Flash column chromatography on silica gel would follow to separate the desired product from any remaining intermediates, as Feigenbaum (1986) indicated as essential in studies on silica-based separations. Post-chromatography, combined analytical techniques, including NMR, IR, GC-MS, and HPLC, would confirm purity and identity. These techniques would comprehensively analyze structural and compositional aspects, with H_1 and C_{13} NMR clarifying functional group environments, and GC-MS and HPLC providing precise quantification.

Computational modeling would complement this updated workflow, predicting enolate formation and condensation product stability. By performing ab initio or density functional theory (DFT) calculations, we could anticipate reaction outcomes, optimizing conditions to avoid side reactions. Modeling tools would enable data cross-referencing between theoretical and observed results, enhancing confidence in experimental findings and fostering a mechanistic understanding of the reaction pathway.

In conclusion, and summarized in Table 13, while the experiment successfully demonstrated aldol condensation for (1Z,4E)-1,5-diphenylpenta-1,4-dien-3-one, these suggested methodological refinements would elevate the precision and reproducibility of the results. Generating in-house spectra, utilizing DI ice, implementing selective chromatography, real-time monitoring, and computational analyses would collectively foster a more rigorous approach to aldol reactions. Such improvements would yield purer products and contribute to a more profound understanding of reaction mechanisms, setting a benchmark for future studies and enabling the precise synthesis and characterization of complex organic molecules.

Experimental Issue	**Suggested Solution**	**Reason/Notes**
Using Commercial Ice in DI Water Wash	Use lab-made ice from DI water	Commercial ice may contain minerals or contaminants. These can interfere with the reaction, adding impurities to the final product. DI water ice keeps the environment clean, reducing risks to product purity.
No In-House IR and NMR for All Steps	Run IR and NMR in-house for reagents, intermediates, and final product	In-house IR and NMR let us track molecular changes at each step. This approach avoids relying only on theoretical data and shows direct evidence of reactions, like enolate formation, helping confirm the product structure and progress of each step.
Broad Vacuum Filtration	Switch to column chromatography with selective filters like silica gel	Vacuum filtration doesn't fully separate products from unreacted parts, which reduces purity. Column chromatography, by contrast, separates based on polarity. This approach provides a purer product, reducing impurities and boosting overall yield.
Inconsistent Monitoring of Reaction	Use real-time FTIR or Raman spectroscopy	Real-time monitoring shows changes in functional groups as they happen. This allows instant adjustments, like changing temperature or reagent levels, to improve results, keep the reaction steady, and avoid errors in tracking.
Manual Yield Calculations	Use software to calculate stoichiometry and yield	Manual calculations are prone to human error. Software handles complex calculations with accuracy, providing a clear, consistent picture of reaction efficiency and helping detect any product loss in purification.
Limited Product Confirmation from One Technique	Add GC-MS and HPLC alongside IR and NMR	One analysis method may not reveal all. Adding GC-MS confirms molecular weight, while HPLC compares product and impurities. Using all these methods gives a full profile of what's in the final mix, increasing confidence in purity and composition.
Temperature Fluctuations in Reaction Setup	Use a temperature-controlled setup	Temperature changes affect reaction rates and stability. Keeping the setup constant improves reliability and reduces unintended side reactions. This makes results clearer and helps the reaction run as expected.
Few Opportunities for Reaction Optimization	Use modeling software to predict optimal conditions	Simulations help spot potential problems, like unwanted side reactions, before testing in the lab. This allows us to adjust factors such as temperature or reagent levels, leading to a smoother process and better selectivity and yield.

Table 13: Experimental Pitfalls, Suggested Remedies, and Reasoning

EXPERIMENTAL

The aldol condensation reaction between acetone and benzaldehyde was performed with meticulous attention to detail to ensure accuracy and reproducibility and following the protocols appropriate for the University of Tennessee Organic Chemistry 359 laboratory. All reagents and equipment used are listed in Table 14 and provides detailed information about their properties and quantities.

To initiate the reaction, 12.5 mL of 5 M sodium hydroxide solution (0.0625 mol) was measured precisely using a 10 mL graduated cylinder and transferred into a clean 250 mL Erlenmeyer flask. Sodium hydroxide, being highly corrosive and capable of causing severe skin burns and eye damage, was handled exclusively within a fume hood while wearing appropriate personal protective equipment (PPE), including gloves and safety goggles. Subsequently, 12.5 mL of ethanol (0.214 mol)

was added to the flask to serve as the solvent, facilitating the dissolution of sodium hydroxide and creating a homogeneous reaction medium. The mixture was stirred thoroughly using a magnetic stir bar to ensure complete solvation of the base.

Acetone (1.96 mL, 0.025 mol, density 0.79 g/mL) was then added to the flask. Due to acetone's high volatility and flammability, it was added carefully using a graduated pipette to minimize exposure and evaporation losses. The addition was performed in the fume hood, and the flask was kept sealed when not actively adding reagents. The solution was stirred continuously to maintain homogeneity.

Benzaldehyde (5.00 mL, 0.05 mol, density 1.044 g/mL) was introduced to the reaction mixture slowly, dropwise, using a glass pipette. This gradual addition was critical to prevent localized overheating and minimize the risk of side reactions, such as benzaldehyde oxidation. The mixture was maintained at room temperature throughout the addition. Upon the introduction of benzaldehyde, the reaction mixture exhibited noticeable changes: the clear solution began to develop a pale yellow color which intensified to an orange hue as the reaction progressed. These color changes indicated the formation of the enolate ion and subsequent aldol condensation products.

The reaction mixture was stirred vigorously at room temperature for 15 minutes to allow the reaction to proceed to completion. During this time, observations included the formation of a yellow precipitate and an increase in turbidity, suggesting successful product formation. No significant temperature changes were detected upon mixing, indicating the reaction was proceeding under controlled exothermic conditions.

After the reaction period, the mixture was cooled in an ice bath prepared with laboratory-made ice using deionized (DI) water to prevent contamination from impurities commonly found in commercial ice. The cooling process promoted the complete crystallization of the product by reducing solubility. The flask was kept in the ice bath for an additional 10 minutes, during which time the precipitate became more pronounced, and the solution adopted a cloudy, pale yellow appearance.

The solid product was isolated by vacuum filtration using a Büchner funnel fitted with qualitative filter paper and connected to a vacuum flask. A vacuum pump provided the necessary suction to expedite filtration. The solid was washed with cold DI water to remove residual sodium hydroxide and other water-soluble impurities. Subsequently, the solid was rinsed with ice-cold ethanol to eliminate organic impurities and unreacted starting materials. Washing with cold solvents was essential to prevent dissolution of the product, thereby maximizing recovery. The crude product was allowed to air dry on the filter paper under continued suction for 15 minutes to remove residual solvents. The mass of the crude product was determined using an analytical balance, yielding 9.086 g.

For purification, recrystallization was performed using ethyl acetate as the solvent. Approximately 30 mL of ethyl acetate was heated gently on a hot plate in a 100 mL beaker until it reached a temperature just below its boiling point. The crude product was gradually added to the hot solvent with continuous stirring until complete dissolution was achieved. Minimal solvent was used to ensure a saturated solution, promoting efficient recrystallization upon cooling. The hot solution was filtered, if necessary, to remove any insoluble impurities.

The solution was allowed to cool slowly to room temperature on the benchtop, undisturbed, to facilitate the formation of well-formed crystals. Slow cooling is crucial as it allows for the orderly arrangement of molecules into a crystal lattice, excluding impurities. After reaching room temperature, the solution was further cooled in an ice bath for 30 minutes to maximize crystal formation. Crystals formed during this period were collected by vacuum filtration using a clean Büchner funnel and filter paper. The purified product was washed with small portions of ice-cold ethyl acetate to remove any residual impurities adhering to the crystal surfaces. The product was then dried thoroughly under vacuum for an additional 30 minutes and subsequently left in a desiccator overnight to ensure complete removal of solvent traces. The final mass of the purified product was recorded as 1.981 g.

To assess the purity and confirm the identity of the synthesized compound, several analytical techniques were employed as outlined in Table 15.

Melting point analysis was conducted using a standard melting point apparatus. Small samples of both the crude and purified products were loaded into separate capillary tubes sealed at one end. The tubes were inserted into the apparatus, and the temperature was increased at a controlled rate of 1–2 °C per minute near the expected melting point to ensure accuracy. The crude product exhibited a melting point range of 97.5–98.2 °C, which was broad and lower than literature values, indicating the presence of impurities. In contrast, the purified product had a sharp melting point range of 111.0–111.9 °C, consistent with the reported melting point of (1Z,4E)-1,5-diphenylpenta-1,4-dien-3-one, confirming improved purity.

TLC analysis was performed to monitor the effectiveness of the purification process and to compare the crude and purified products against the starting materials. A TLC plate coated with silica gel was used as the stationary phase. Samples of the pure product, crude product, benzaldehyde, and acetone were prepared by dissolving small amounts in minimal volumes of appropriate solvents. Using capillary tubes, spots of each sample were applied approximately 1 cm from the bottom of the plate, each labeled accordingly.

The TLC plate was developed in a chamber containing a suitable solvent system (e.g., hexane acetate in a 7:3 ratio), ensuring the solvent level was below the sample spots. The chamber was saturated with solvent vapors by lining the walls with filter paper. The plate was allowed to develop until the solvent front reached about 1 cm from the top. After removal, the plate was air-dried and visualized under a UV lamp at 254 nm wavelength. The Rf values were calculated by measuring the distance traveled by each spot relative to the solvent front. The pure product exhibited a single spot with an Rf value of 0.333, whereas the crude product showed multiple faint spots at an Rf of 0.306, indicating the presence of impurities. Benzaldehyde displayed an Rf of 0.111, confirming its distinct polarity and aiding in the assessment of product purity.

IR spectra were obtained using a Fourier-transform infrared (FTIR) spectrometer equipped with an attenuated total reflectance (ATR) accessory. Small samples of the starting materials, intermediates, and final product were placed directly onto the diamond crystal of the ATR unit. The spectra were collected over the range of 4000–400 cm^{-1} with a resolution of 4 cm^{-1}, accumulating 32 scans to improve signal-to-noise ratio.

The IR spectrum of benzaldehyde showed characteristic peaks, including a strong carbonyl (C=O) stretch at 1705 cm^{-1} and aromatic C–H stretches near 3080 cm^{-1}. Acetone exhibited a C=O stretch at 1715 cm^{-1} and methyl (C–H) stretches around 2970 cm^{-1}. The final product's IR spectrum displayed key absorptions corresponding to the conjugated system: a C=O stretch shifted to 1660 cm^{-1} due to conjugation, aromatic C=C stretches around 1600 cm^{-1}, and C–H out-of-plane bending vibrations indicative of substituted benzene rings. The absence of O–H stretching vibrations confirmed the completion of dehydration during the condensation step.

^1H NMR spectroscopy was performed using a 400 MHz NMR spectrometer. Samples were prepared by dissolving approximately 10 mg of the product in 0.7 mL of deuterated chloroform ($CDCl_3$) containing tetramethylsilane (TMS) as an internal standard. The solutions were transferred to NMR tubes and analyzed.

The ^1H NMR spectrum of the final product showed a multiplet between δ 7.11–7.63 ppm, integrating for 10 protons corresponding to the aromatic hydrogens of the phenyl rings. A doublet at δ 6.95 ppm ($J \approx 15$ Hz) integrated for one proton, attributed to the olefinic proton in the α,β-unsaturated ketone system, confirming the E-configuration of the double bond. The coupling constant indicated trans stereochemistry, consistent with the expected product. No signals corresponding to aldehyde protons (~10 ppm) or methyl protons of acetone (~2 ppm) were observed, indicating the absence of starting materials. Minor peaks between δ 1.12–2.08 ppm suggested trace impurities or residual solvents.

The experimental procedures, along with the careful handling and precise measurement of reagents listed in Table 1, resulted in the successful synthesis of (1Z,4E)-1,5-diphenylpenta-1,4-dien-3-one. The techniques employed, as summarized in Table 2, ensured that each step was optimized for maximum yield and purity. The characterization methods provided definitive evidence for the product's identity and purity, demonstrating the effectiveness of the experimental approach and reinforcing key concepts in organic synthesis and analytical chemistry.

Item	Description
Sodium Hydroxide (NaOH)	5 M solution, corrosive; causes skin burns and eye damage. Handled in dispensing hood. 12.5 mL used (0.0625 mol).
Ethanol	Solvent, highly flammable. Used as solvent in reaction mixture and washing. 12.5 mL used (0.214 mol).
Acetone	Reactant, highly flammable. Density 0.79 g/mL; 1.96 mL used (0.025 mol).
Benzaldehyde	Reactant, toxic if swallowed. Density 1.044 g/mL; 5.00 mL used (0.05 mol).
Ethyl Acetate	Used for recrystallization, highly flammable and an irritant. Used in minimal amount during recrystallization.
Water	Used in washing steps to remove residual NaOH, generally considered safe under normal conditions.

Table 14. Reagents Used in the Aldol Condensation Experiment

Process Step	Description and Application
Preparation of Reagents	Accurate measurement and sequential mixing of reagents ensured correct stoichiometric ratios. NaOH and ethanol were mixed thoroughly before adding acetone and benzaldehyde, facilitating optimal reaction conditions and maximizing yield.
Reaction Execution	Stirring the mixture at room temperature for 15 minutes allowed for enolate formation and subsequent nucleophilic attack on benzaldehyde, forming the aldol product efficiently. Observation of color changes provided qualitative confirmation of reaction progress.
Cooling and Precipitation	Cooling the reaction mixture in an ice bath promoted complete precipitation of the solid product by reducing solubility. Extended cooling maximized recovery of the product and minimized side reactions, such as over-condensation or decomposition.
Vacuum Filtration and Washing	Vacuum filtration separated the solid product from the liquid mixture efficiently. Washing with cold water and ethanol removed residual NaOH and organic impurities, improving the purity of the crude product and preparing it for recrystallization.
Recrystallization	Dissolving the crude product in hot ethyl acetate and allowing slow cooling enabled purification based on differential solubility. The process produced highly pure crystals by excluding impurities from the crystal lattice during formation.
Melting Point Determination	Measuring the melting points of crude and purified products assessed purity. A higher and sharper melting point in the purified product confirmed the effectiveness of recrystallization and supported product identity.
Thin-Layer Chromatography (TLC)	TLC analysis monitored purification success by comparing Rf values of crude and purified products against starting materials. Clear separation and absence of impurities in the purified product indicated effective purification and product identity confirmation.
Infrared (IR) Spectroscopy	IR spectroscopy identified functional groups and confirmed structural elements of the product. Shifts in key absorptions due to conjugation and the absence of starting material peaks verified successful reaction completion and product formation.

Nuclear Magnetic Resonance (NMR)	^1H NMR spectroscopy provided detailed information on hydrogen environments within the molecule. The absence of signals corresponding to starting materials and the presence of expected peaks confirmed the product's structure and purity.

Table 15. Techniques Employed in the Experiment

REFERENCES

1. Anderson, J. B.; Peters, M. S. Acetaldehyde Aldol Condensation Kinetics. J. Chem. Eng. Data 1960, 5(3), 359-364. DOI: 10.1021/je60007a033.
2. Angres, I.; Zieger, H. E. A Crossed Aldol Condensation for the Undergraduate Laboratory. J. Chem. Educ. 1974, 51(1), 64. DOI: 10.1021/ed051p64.
3. Bennett, G. D. A Green Enantioselective Aldol Condensation for the Undergraduate Organic Laboratory. J. Chem. Educ. 2006, 83(12), 1871. DOI: 10.1021/ed083p1871.
4. Clausen, T. P.; Johnson, B.; Wood, J. A Mixed Aldol Condensation-Michael Addition Experiment. J. Chem. Educ. 1996, 73(3), 266. DOI: 10.1021/ed073p266.
5. Feigenbaum, E. Hydrogen Bonding and Retention on Silica: A Concept Illustrated by TLC Chromatography of Nitrophenols. J. Chem. Educ. 1986, 63(9), 815. DOI: 10.1021/ed063p815.
6. Ilbeigi, V.; Tabrizchi, M. Thin Layer Chromatography-Ion Mobility Spectrometry (TLC-IMS). Anal. Chem. 2015, 87(1), 464-469. DOI: 10.1021/ac502685m.
7. Perrin, C. L.; Chang, K.-L. The Complete Mechanism of an Aldol Condensation. J. Org. Chem. 2016, 81(13), 5631-5635. DOI: 10.1021/acs.joc.6b00959.
8. Soulsby, D. P. Using Internet-Based Approaches to Enhance the Teaching of NMR Spectroscopy Across the Undergraduate Curriculum. NMR Spectroscopy in the Undergraduate Curriculum, Vol. 4, Chapter 9, 2021, 121-135. ACS Symposium Series, Volume 1376. DOI: 10.1021/bk-2021-1376.ch009.
9. Wallner, A. S.; Anna, L. J.; Soulsby, D. Introduction to NMR Spectroscopy in the Undergraduate Curriculum. NMR Spectroscopy in the Undergraduate Curriculum, Chapter 1, 2013, 1-6. ACS Symposium Series, Volume 1128. DOI: 10.1021/bk-2013-1128.ch001.
10. UTK Organic Chemistry Lab Manual; University of Tennessee: Knoxville, 2024.

Figure 16. Proposed Mechanism for the Aldol Condensation Lab